

**A mutation in the intracellular loop III/IV of mosquito sodium channel synergizes the effect of mutations in helix IIS6 on pyrethroid resistance**

Lingxin Wang, Yoshiko Nomura, Yuzhe Du, Nannan Liu, Boris S. Zhorov, Ke Dong

Department of Entomology, Genetics and Neuroscience Programs, Michigan State University, East Lansing, MI, USA (L.W., Y.N., Y.D,K.D.)

Department of Entomology and Plant Pathology; Auburn University, Auburn, Alabama, USA (N.L.)

Department of Biochemistry and Biomedical Sciences, McMaster University, Hamilton, Ontario, Canada (B.S.Z.)

Sechenov Institute of Evolutionary Physiology & Biochemistry, Russian Academy of Sciences, St. Petersburg (B.S.Z.)

MOL #94730

**Running title:** Synergism of sodium channel mutations on pyrethroid action

\*Corresponding author. Email: [dongk@cns.msu.edu](mailto:dongk@cns.msu.edu); Telephone: 517-432-2034; Fax: 517-353-4354

Number of text pages:

Number of tables: 1

Number of figures: 6

Number of references: 43

Number of words in Abstract: 236

Number of words in Introduction: 666

Number of words in Discussion: 1066

A list of nonstandard abbreviations: AaNa<sub>v</sub>, mosquito sodium channel; L45, linker connecting S4 and S5 of sodium channels; LIII-IV, the cytoplasmic loop linking domains III and IV; PyR1, pyrethroid receptor site1; PyR2, pyrethroid receptor site 2.

## Abstract

Activation and inactivation of voltage-gated sodium channels are critical for proper electrical signaling in excitable cells. Pyrethroid insecticides promote activation and inhibit inactivation of sodium channels, resulting in prolonged opening of sodium channels. They preferably bind to the open state of the sodium channel by interacting with two distinct receptor sites, PyR1 and PyR2, formed by the interfaces of domains II/III and I/II, respectively. Specific mutations in PyR1 or PyR2 confer pyrethroid resistance in various arthropod pests and disease vectors. Recently, a unique mutation, N<sup>1575</sup>Y, in the cytoplasmic loop linking domains III and IV (LIII-IV) was found to co-exist with a PyR2 mutation, L<sup>1014</sup>F in IIS6, in pyrethroid-resistant populations of *Anopheles gambiae*. To examine the role of this mutation in pyrethroid resistance, N<sup>1575</sup>Y alone or N<sup>1575</sup>Y+L<sup>1014</sup>F were introduced into an *Aedes aegypti* sodium channel, AaNa<sub>v</sub>1-1, and the mutants were functionally examined in *Xenopus* oocytes. N<sup>1575</sup>Y did not alter AaNa<sub>v</sub>1-1 sensitivity to pyrethroids. However, the N<sup>1575</sup>Y+L<sup>1014</sup>F double mutant was more resistant to pyrethroids than the L<sup>1014</sup>F mutant channel. Further mutational analysis showed that N<sup>1575</sup>Y could also synergize the effect of L<sup>1014</sup>S/W, but not L<sup>1014</sup>G or other pyrethroid-resistant mutations in IS6 or IIS6. Computer modeling predicts that N<sup>1575</sup>Y allosterically alters PyR2 via a small shift of IIS6. Our findings provide the molecular basis for the co-existence of N<sup>1575</sup>Y with L<sup>1014</sup>F in pyrethroid resistance, and suggest an allosteric interaction between IIS6 and LIII-IV in the sodium channel.

## Introduction

Voltage-gated sodium channels are responsible for the rapidly rising phase of action potentials (Catterall, 2012). Because of their critical role in membrane excitability, sodium channels are the primary target site of a variety of naturally occurring and synthetic neurotoxins, including pyrethroid insecticides (Catterall et al., 2007). Pyrethroids promote activation and inhibit inactivation of sodium channels resulting in prolonged opening of sodium channels (Narahashi, 1996; Vijverberg et al., 1982). Pyrethroid insecticides possess high insecticidal activities and low mammalian toxicity and represent one of the most powerful weapons in the global fight against malaria and other arthropod-borne human diseases. However, the efficacy of pyrethroids is undermined as a result of emerging pyrethroid resistance in arthropod pest and disease vectors. One major resistance mechanism is known as knockdown resistance (*kdr*), which arises from mutations in the sodium channel (Dong et al., 2014; Rinkevich et al., 2013; Soderlund, 2005).

The pore-forming  $\alpha$ -subunit of the sodium channel is composed by four homologous domains (I-IV), each having six transmembrane segments (S1-S6) connected by intracellular and extracellular loops. The S1-S4 segments in each domain serve as the voltage-sensing module, whereas the S5 and S6 segments and the loops connecting them function as the pore-forming module. In response to membrane depolarization, the S4 segments move outward, initiating conformational changes which lead to pore opening and subsequent inactivation of sodium channels. Short intracellular linkers between the S4 and S5 segments (L45) transmit the movements of the voltage sensing modules to the S6 segments during channel opening and closing. Fast inactivation is achieved by the movement of an inactivation gate formed mainly by

the IFM motif in the short intracellular linker connecting domains III and IV, which physically occludes the open pore.

In the recent years, using X-ray structures of a bacterial potassium channel KcsA (Doyle et al., 1998), the mammalian voltage-gated potassium channel K<sub>v</sub>1.2 crystallized in the open state (Long et al., 2005) and a bacterial sodium channel, Na<sub>v</sub>Ab, crystallized in the closed state (Payandeh et al., 2011) as templates, homology models of eukaryotic sodium channels have been developed to predict binding sites of sodium channel neurotoxins (Du et al., 2013; Lipkind and Fozzard, 2005; O'Reilly et al., 2006; Tikhonov and Zhorov, 2007; Tikhonov and Zhorov, 2012). Mutational analyses coupled with computer modeling show that pyrethroids bind to two analogous receptor sites. PyR1 is formed by residues from helices IIL45, IIS5, and IIS6 (O'Reilly et al., 2006), whereas PyR2 is formed by residues from helices IL45, IS5, IS6, and IIS6 (Du et al., 2013). Binding of pyrethroid molecules at the two sites is believed to effectively trap the sodium channel in the open state, resulting in the prolonged opening of sodium channels (Du et al., 2013).

The most frequent *kdr* mutation in arthropod pests and disease vectors is a leucine to phenylalanine (L<sup>1014</sup>F in the house fly sodium channel) in IIS6, which is also known as L<sup>2i16</sup>F using the nomenclature that is universal for sodium channels and other P-loop ion channels (Du et al., 2013; Zhorov and Tikhonov, 2004) (Figure 1). The L<sup>2i16(1014)</sup>F mutation has been detected in the malaria vector *Anopheles* mosquito species in many regions around the world (Enayati et al., 2003; Karunaratne et al., 2007; Martinez-Torrez et al., 1998). Recently, a new sodium channel mutation N<sup>1575</sup>Y was reported in the malaria mosquito, *Anopheles gambiae*, in Africa (Jones et al., 2012). The N<sup>1575</sup>Y mutation is located in the intracellular loop connecting domains III and IV

(LIII-IV) (Figure 1). Intriguingly, the N<sup>1575</sup>Y mutation was only found in conjunction with L<sup>2i16(1014)</sup>F: no mosquito individuals were detected harboring only the N<sup>1575</sup>Y mutation (Jones et al., 2012). Interestingly, pyrethroid bioassays indicate that mosquitoes carrying the double mutations L<sup>2i16(1014)</sup>F+N<sup>1575</sup>Y are more resistant to permethrin than mosquitoes carrying only the L<sup>2i16(1014)</sup>F mutation (Jones et al., 2012). However, whether the N<sup>1575</sup>Y mutation confers pyrethroid resistance has not been functionally confirmed yet. In this study, we conducted site-directed mutagenesis, functional analysis in *Xenopus* oocytes, and computer modelling to investigate the role of N<sup>1575</sup>Y in pyrethroid resistance.

## Materials and Methods

### *Site-directed mutagenesis*

Because sodium channels from *An. gambiae* have not been successfully expressed in the *Xenopus* oocyte expression system for functional characterization, we used a mosquito sodium channel, AaNa<sub>v</sub>1-1, from *Ae. aegypti* to generate all mutants used in this study. The *kdr* mutations that are explored in this study are located in regions that are highly conserved between sodium channels from *An. gambiae* and *Ae. aegypti* (Supplemental Figure 1). Site-directed mutagenesis was performed by Polymerase Chain Reaction (PCR) using Pfu Turbo DNA polymerase (Stratagene, La Jolla, CA). All mutagenesis results were confirmed by DNA sequencing.

### *Expression of AaNa<sub>v</sub> sodium channels in Xenopus oocytes*

The procedures for oocyte preparation and cRNA injection are identical to those described previously (Tan et al., 2002a). For robust expression of AaNa<sub>v</sub>1-1 sodium channels, cRNAs were co-injected into oocytes with *Ae. aegypti* *TipE* cRNA (1:1 ratio), which enhances the expression of sodium channels in oocytes.

### *Electrophysiological recording and analysis.*

The voltage dependence of activation and inactivation was measured using the two-electrode voltage clamp technique. Methods for two-electrode recording and data analysis were identical to those described previously (Tan et al., 2002b).

The voltage dependence of sodium channel conductance ( $G$ ) was calculated by measuring the peak current at test potentials ranging from -80 mV to +65 mV in 5-mV increments and divided by  $(V - V_{rev})$ , where  $V$  is the test potential and  $V_{rev}$  is the reversal potential for sodium

ions. Peak conductance values were normalized to the maximal peak conductance ( $G_{\max}$ ) and fitted with a two-state Boltzmann equation of the form  $G/G_{\max} = [1 + \exp(V - V_{1/2})/k]^{-1}$ , in which  $V$  is the potential of the voltage pulse,  $V_{1/2}$  is the voltage for half-maximal activation, and  $k$  is the slope factor.

The voltage dependence of sodium channel inactivation was determined by using 100-ms inactivating prepulses ranging from -120 mV to 10 mV in 5-mV increments from a holding potential of -120 mV, followed by test pulses to -10 mV for 20 ms. The peak current amplitude during the test depolarization was normalized to the maximum current amplitude and plotted as a function of the prepulse potential. Data were fitted with a two-state Boltzmann equation of the form  $I/I_{\max} = [1 + (\exp(V - V_{1/2})/k)]^{-1}$ , in which  $I$  is the peak sodium current,  $I_{\max}$  is the maximal current evoked,  $V$  is the potential of the voltage prepulse,  $V_{1/2}$  is the half-maximal voltage for inactivation, and  $k$  is the slope factor. Sodium current decay was analyzed by fitting the decaying part of current traces with a single exponential function.

#### *Measurement of tail currents induced by pyrethroids*

The method for application of pyrethroids in the recording system was identical to that described previously (Tan et al., 2002b). The effects of pyrethroids were measured 10 min after their application. The pyrethroid-induced tail current was recorded during a 100-pulse train of 5-ms step depolarizations from -120 to 0 mV with 5-ms interpulse intervals (Vais et al., 2000). The percentage of channels modified by pyrethroids was calculated using the equation  $M = \{I_{\text{tail}}/(E_h - E_{\text{Na}})/[I_{\text{Na}}/(E_t - E_{\text{Na}})]\} \times 100$  (Tatebayashi and Narahashi, 1994), where  $I_{\text{tail}}$  is the maximal tail current amplitude,  $E_h$  is the potential to which the membrane is repolarized,  $E_{\text{Na}}$  is the reversal potential for sodium current determined from the current-voltage curve,  $I_{\text{Na}}$  is the

amplitude of the peak current during depolarization before pyrethroid exposure, and  $E_t$  is the potential of step depolarization.

### *Molecular modeling*

We used the  $K_v1.2$ -based model of the open AaNa $_v1-1$  channel with deltamethrin bound into PyR2 (Du et al., 2013) as a starting point to generate models of mutants with deltamethrin. Because pyrethroids preferably bind to sodium channels in the open state, the X-ray structure of the open potassium channel  $K_v1.2$  (Long et al., 2005) was used as template in this study and also in previous models of insect sodium channels with pyrethroids (Du et al., 2013; O'Reilly et al., 2006; O'Reilly et al., 2014). The selectivity-filter region, which is substantially different between potassium and sodium channels, was not included in the models because it is far from the pyrethroid receptors (O'Reilly et al., 2006; Usherwood et al., 2007). Homology modeling and ligand docking were performed using the ZMM program ([www.zmmsoft.com](http://www.zmmsoft.com)). Monte Carlo-minimization protocol (Li and Scheraga 1987) was used for energy optimization as described in Du et al. (2013) and Garden and Zhorov (2010). The complexes were visualized with PyMol.

### *Chemicals*

Deltamethrin was kindly provided by Bhupinder Khambay (Rothamsted Research, Harpenden, UK). Deltamethrin was dissolved in dimethyl sulfoxide (DMSO). The working concentration was prepared in ND96 recording solution immediately prior to experiments. The concentration of DMSO in the final solution was <0.5%, which had no effect on the function of sodium channels.

### *Statistical analysis*

MOL #94730

Results are reported as mean  $\pm$  SEM. Statistical significance was determined by using one-way analysis of variance (ANOVA) with Scheffe's post hoc analysis, and significant values were set at  $p < 0.05$ .

## Results

### **N<sup>1575</sup>Y does not alter the gating properties of AaNa<sub>v</sub>1-1 channels**

The N<sup>1575</sup>Y mutation is located in LIII-IV, which is important for fast inactivation of sodium channels (Catterall, 2002; Goldin, 2003). To determine whether the N<sup>1575</sup>Y mutation alters inactivation kinetics, we introduced this mutation into AaNa<sub>v</sub>1-1 and expressed both AaNa<sub>v</sub>1-1 and mutant channels in *Xenopus* oocytes. Like AaNa<sub>v</sub>1-1, the mutant channel produced sufficient sodium currents for functional analysis (Figure 2). AaNa<sub>v</sub>1-1 and N<sup>1575</sup>Y channels had similar rates of sodium current decay over the entire range of voltages examined, indicating that the mutation did not alter the kinetics of fast inactivation (Figure 2). Furthermore, the mutation did not alter the voltage-dependence of either activation or inactivation (Table 1).

Because the N<sup>1575</sup>Y mutation co-exists with the L<sup>2i16(1014)</sup>F mutation in *An. gambiae* (Jones et al., 2012), the N<sup>1575</sup>Y change was also introduced into AaNa<sub>v</sub>1-1 carrying the L<sup>2i16(1014)</sup>F mutation, which was generated in a previous study (Du et al., 2013), to create a double mutation construct L<sup>2i16(1014)</sup>F+N<sup>1575</sup>Y. Similarly, L<sup>2i16(1014)</sup>F and L<sup>2i16(1014)</sup>F+N<sup>1575</sup>Y channels exhibited similar fast inactivation kinetics compared to AaNa<sub>v</sub>1-1 (Figure 2). The voltage-dependences of activation and inactivation of both mutant channels were also similar to those of the AaNa<sub>v</sub>1-1 channel (Table 1).

### **N<sup>1575</sup>Y enhances L<sup>2i16(1014)</sup>F-mediated resistance to pyrethroids, but does not confer pyrethroid resistance alone**

To examine the effect of the N<sup>1575</sup>Y mutation on the sensitivity of AaNa<sub>v</sub>1-1 channels to pyrethroids, we compared the sensitivities of AaNa<sub>v</sub>1-1, N<sup>1575</sup>Y, L<sup>2i16(1014)</sup>F and L<sup>2i16(1014)</sup>F+N<sup>1575</sup>Y channels to both a type I pyrethroid, permethrin, and type II pyrethroid, deltamethrin. The

percentage of sodium channel modification by pyrethroids was determined by measuring pyrethroid-induced tail currents upon repolarization in voltage-clamp experiments. The effect of permethrin on the N<sup>1575</sup>Y channel was similar to that on AaNa<sub>v</sub>1-1 (Figure 3A and B). However, the permethrin-induced tail current was reduced by the L<sup>2i16(1014)</sup>F mutation and more drastically by L<sup>2i16(1014)</sup>F+N<sup>1575</sup>Y double mutations (Figure 3B-D). Furthermore, analysis of the dose response curves of modification of AaNa<sub>v</sub>1-1 and the three mutant channels by permethrin and deltamethrin showed that the L<sup>2i16(1014)</sup>F mutant channel was about 8-fold more resistant to permethrin than the AaNa<sub>v</sub>1-1 channel (Figure 3E) and the L<sup>2i16(1014)</sup>F channel was 14-fold more resistant to deltamethrin than the AaNa<sub>v</sub>1-1 channel (Figure 3F). Remarkably, the L<sup>2i16(1014)</sup>F+N<sup>1575</sup>Y channel was 80-fold more resistant to permethrin and 53-fold more resistant to deltamethrin than the wild type channel. Therefore, the N<sup>1575</sup>Y mutation increased resistance to permethrin and deltamethrin by 9.8-fold and 3.4-fold, respectively, when combined with the L<sup>2i16(1014)</sup>F+N<sup>1575</sup>Y mutation. However, the N<sup>1517</sup>Y mutation had no effect on channel sensitivity to either pyrethroid.

### **N<sup>1575</sup>Y enhances pyrethroid resistance caused by L<sup>2i16(1014)</sup>S/W mutations**

Our results above indicate that the N<sup>1575</sup>Y mutation imposes a synergistic effect on pyrethroid resistance caused by the L<sup>2i16(1014)</sup>F mutation. To see whether such synergism extends to pyrethroid resistance caused by other *kdr* mutations identified in pyrethroid resistant mosquitoes, we examined three additional *kdr* mutations, L<sup>2i16(1014)</sup>FS/C/W, which have been reported in various mosquito species (Kasai et al., 2011; Kawada et al., 2009; Kim et al., 2007; Luleyap et al., 2002; Ranson et al., 2000; Singh et al., 2010; Stump et al., 2004; Tan et al., 2012; Verhaeghen et al., 2010; Wang et al., 2012). These mutations did not affect the

voltage dependence of activation or inactivation of AaNa<sub>v</sub>1-1 channels either alone or in conjunction with the N<sup>1575</sup>Y mutation (Table 1). Consistent with results from a previous study (Du et al., 2013), the L<sup>2i16(1014)</sup>S channel was 6.7-fold and 9-fold more resistance to permethrin and deltamethrin, respectively, than the AaNa<sub>v</sub>1-1 channel (Figure 4A and B). The L<sup>2i16(1014)</sup>S+N<sup>1575</sup>Y double mutant channel was 58-fold and 32-fold more resistant to permethrin and deltamethrin, respectively, than the AaNa<sub>v</sub>1-1 channel (Figure 4A and B). Similarly, the L<sup>2i16(1014)</sup>W mutant channel was more resistant to permethrin and deltamethrin than the AaNa<sub>v</sub>1-1 channel by about 9.7-fold and 7-fold, respectively (Figure 4C and D), and introduction of N<sup>1575</sup>Y mutation into the L<sup>2i16(1014)</sup>W channel caused an additional 10.5-fold and 13-fold resistance to permethrin and deltamethrin (101.8 and 91-fold resistance to permethrin and deltamethrin versus wild-type), respectively (Figure 4C and D). Another *kdr* mutation at the same position, L<sup>2i16(1014)</sup>C, also caused 3.5 and 4.2 fold reduction in AaNa<sub>v</sub>1-1 sensitivity to permethrin and deltamethrin, respectively (Supplemental Figure 2). However, the L<sup>2i16(1014)</sup>C+N<sup>1575</sup>Y double mutant did not produce sufficient sodium currents in oocytes for further functional analysis.

### **N<sup>1575</sup>Y did not enhance pyrethroid resistance caused by another *kdr* mutation in IIS6, but in PyR1**

Next we examined another *kdr* mutation in IIS6, V<sup>2i18(1016)</sup>G, which is detected in pyrethroid-resistant populations of *Ae. aegypti* (Saavedra-Rodriguez et al., 2007). Although all located in IIS6, L<sup>2i16(1014)</sup>F/S/W and V<sup>2i18(1016)</sup>G belong to PyR2 and PyR1, respectively (Du et al., 2013). We introduced the N<sup>1575</sup>Y mutation into the V<sup>2i18(1016)</sup>G channel construct, which was available from a previous study (Du et al., 2013). Consistent with the finding from the previous study, the

V<sup>2i18(1016)</sup>G mutation significantly reduced AaNav<sub>v</sub>1-1 channel sensitivity to both permethrin and deltamethrin (Figure 5B and C), but the addition of the N<sup>1575</sup>Y mutation did not further enhance the level of resistance to pyrethroids (Figure 5B and C).

### **N<sup>1575</sup>Y did not enhance pyrethroid resistance caused by other mutations in PyR2**

Many *kdr* mutations are located within the two pyrethroid-binding sites and/or are involved in regulating channel kinetics and voltage-dependent gating (Dong et al., 2014). N<sup>1575</sup>Y is not located in either of the pyrethroid receptor sites and does not affect inactivation kinetics or channel gating (Figure 2; Table 1). Therefore, we hypothesize that N<sup>1575</sup>Y exerts its effect by allosterically altering one of the pyrethroid binding sites. The alteration *per se* must be small because N<sup>1575</sup>Y alone does not affect the action of pyrethroids except in the presence of another resistance-associated mutation at L<sup>2i16(1014)</sup>. Since the N<sup>1575</sup>Y mutation enhances the effect of mutations at L<sup>2i16(1014)</sup>, but not at V<sup>2i18(1016)</sup>G, we then focused on residues in PyR2 to determine the extent of the N<sup>1575</sup>Y-mediated synergism. In the PyR2 model (Du et al., 2013), the side chain of L<sup>2i16(1014)</sup> is directed towards the pyrethroid-sensing residue L<sup>1i18</sup> in IS6 (Figure 6A). Consistent with previous findings (Du et al., 2013), L<sup>1i18</sup>G reduced AaNav<sub>v</sub>1-1 channel sensitivity to permethrin and deltamethrin. However, the double mutation L<sup>1i18</sup>G+N<sup>1575</sup>Y was not more resistant to pyrethroids than the single mutant, L<sup>1i18</sup>G or S<sup>1i29</sup>A (Figure 5B and C). Furthermore, we introduced two additional substitutions, L<sup>1i18</sup>F and L<sup>1i18</sup>W, into both AaNav1-1 and N<sup>1575</sup>Y channels. Like L<sup>1i18</sup>G, both substitutions reduced the action of pyrethroids (Fig. 5B and C) and the N<sup>1575</sup>Y mutation did not enhance pyrethroid resistance caused by either mutation (Fig. 5B and C). In addition, S<sup>1i29</sup> at the end of IS6 is predicted to approach the alpha-cyano group of deltamethrin and favorably contribute to ligand-channel interactions (Figure 6A-

B). Here we showed that  $S^{1i29}A$  decreased channel sensitivity to pyrethroids (Figure 5B and C), further supporting the PyR2 model. However, the  $S^{1i29}A+N^{1575}Y$  channel was not more resistant to both pyrethroids than the single  $S^{1i29}A$  mutant. Collectively, these results suggest that the modification of the receptor site by  $N^{1575}Y$  may be  $L^{2i16(1014)}$ -specific. It is possible that unfavorable interactions of the hydrophobic ligand with large aromatic substitutions  $L^{2i16(1014)}F/W$  or hydrophilic substitution  $L^{2i16(1014)}S$  were further reduced by  $N^{1575}Y$ . Thus, we examined a glycine substitution of  $L^{2i16(1014)}$ , i.e.,  $L^{2i16(1014)}G$ , for pyrethroid sensitivity. Like  $L^{2i16(1014)}F/S/W$ , the  $L^{2i16(1014)}G$  substitution reduced the AaNa<sub>v</sub>1-1 channel sensitivity to permethrin and deltamethrin. However, the  $L^{2i16(1014)}G+N^{1575}Y$  double mutant channel was as sensitive as the  $L^{2i16(1014)}G$  channel to both permethrin and deltamethrin (Figure 5B and C). These results suggest that the effect of  $N^{1575}Y$ , potentially causing a small conformational shift in IIS6, on pyrethroid binding is sensitive to the nature of the residue at position 2i16 (1014).

#### **Possible mechanism of synergy between $N^{1575}Y$ and $L^{2i16(1014)}F/S/W$ mutations**

To explore how  $N^{1575}Y$  enhances pyrethroid resistance of AaNa<sub>v</sub>1-1 channels when combined with the  $L^{2i16(1014)}F/S/W$  mutations, but not in wild-type or with the  $L^{2i16}G$  mutation, we compared the model of deltamethrin binding in PyR2 of the wild-type open AaNa<sub>v</sub>1-1 channel and the mutants (Figure 6). PDB format files for the AaNa<sub>v</sub>1-1 channel models are provided in the Data Supplement. In the wild-type channel, deltamethrin favorably interacts with the long flexible side chain of  $L^{2i16(1014)}$  (Figure 6A). Comparison of deltamethrin binding models in the wild-type channel and mutants  $L^{1i18}G$  (Figure 6C) and  $L^{2i16}G$  (Figure 6D) suggests two consequences of the glycine substitutions. First, the favorable interactions of the hydrophobic ligand with the large hydrophobic pyrethroid-sensing residues are lost. Second, there is

MOL #94730

significantly more space in the pyrethroid binding site following mutation of L<sup>2i16</sup> to G. Models of deltamethrin binding in the L<sup>2i16</sup>S, and L<sup>2i16</sup>F mutants show unfavorable interactions between the hydrophilic S<sup>2i16</sup> or the large and inflexible F<sup>2i16</sup> with the hydrophobic ligand (Figure 6E and F). Therefore, we suggest that enhancement of pyrethroid resistance in the presence of the L<sup>2i16(1014)</sup>F/S/W mutations occurs as a result of a slight shift of IIS6. The shift does not affect either the favorable interaction of pyrethroids with L<sup>2i16</sup> or the less sterically constrained interactions of deltamethrin with the L<sup>2i16</sup>G mutation. In contrast, the slight shift of IIS6 likely further deteriorates the energetically unfavorable interactions of deltamethrin with L<sup>2i16(1014)</sup>F/S/W, enhancing pyrethroid resistance in the double mutant.

## Discussion

Identification of naturally occurring mutations in the sodium channel that confer kdr to pyrethroids has greatly advanced our understanding of the molecular mechanisms of kdr and the molecular details of pyrethroid receptor sites (Dong et al., 2014). Emerging evidence suggests that binding of pyrethroids to two distinct pyrethroid receptor sites, PyR1 and PyR2, at two analogous domain interfaces is necessary to trap sodium channels in the open state, which leads to prolonged opening of sodium channels and the toxic effects of pyrethroids *in vivo*. Importantly, many, but not all, kdr mutations that cause pyrethroid resistance are located within the two pyrethroid receptor sites (Dong et al., 2014), and it is not clear how kdr mutations beyond the receptor sites affect pyrethroid sensitivity of sodium channels. In this study, we investigated the role of a pyrethroid resistance-associated mutation, N<sup>1575</sup>Y, which is located in the intracellular loop connecting domains III and IV (outside of PyR1 and PyR2) in pyrethroid resistance. We found that this mutation alone has no effect on the action of pyrethroids on sodium channels, but, enhances pyrethroid resistance caused by the L<sup>2i16(1014)</sup>F/S/W mutations. Based on further mutational analysis and computer modeling, we hypothesize that N<sup>1575</sup> induces a small shift of the transmembrane helix IIS6 resulting in slight deformation of PyR2, which enhances the energetically unfavorable interactions between deltamethrin and the L<sup>2i16(1014)</sup>F/S/W mutations, but does not affect the energetically favorable interactions between pyrethroids and L<sup>2i16(1014)</sup>. These results provide a satisfying explanation for the concurrent existence of N<sup>1575</sup>Y and L<sup>2i16(1014)</sup>F in pyrethroid-resistant mosquito populations.

BLAST searches show that the asparagine residue (equivalent to N<sup>1575</sup> in *An. gambiae*) in this loop sequence is highly conserved among voltage-gated sodium channels. However, N<sup>1575</sup>Y has no effect on the kinetics of fast inactivation, implying that this mutation does not interfere with the docking of the inactivation particle (the motif MFMT in LIII/IV) to its receptor site which is composed of residues in the linkers connecting S4 and S5 of domains III and IV (Goldin, 2003). Our molecular modeling (Fig. 6) predicts that a slight shift of helix IIS6 in the N<sup>1575</sup>Y channel could explain the synergism on pyrethroid resistance between N<sup>1575</sup>Y and specific mutations at L<sup>2i16(1014)</sup>F in IIS6, which is also supported by our mutational analysis (Figs. 3-5). However, we cannot completely rule out the possibility of the N<sup>1575</sup>Y/L<sup>2i16(1014)</sup>F double mutation causing an allosteric effect on the action of pyrethroids without directly involving IIS6.

How a mutation in the intracellular loop between domains III and IV (LIII/IV) can shift helix IIS6 carrying the L<sup>2i16(1014)</sup>F mutation remains speculative. In X-ray structures of both open and closed ion channels, the cytoplasmic parts of the S6 helices approach each other to form the activation gate, and cytoplasmic linkers may also approach each other. We speculate that the asparagine side chain in LIII/IV is involved in specific contacts (likely an H-bond) with LII/III. Replacement of a small asparagine with a much bigger tyrosine in N<sup>1575</sup>Y could cause a change in the mutual disposition of the two linkers, which, in turn, would shift helix IIS6. This predicted small shift in IIS6 by N<sup>1575</sup>Y apparently only alters the action of pyrethroids on L<sup>2i16(1014)</sup>F/S/C/W channels, but not on L<sup>2i16</sup>G and V<sup>2i18(1018)</sup>G channels. This may be because a small distortion of PyR2 upon the N<sup>1575</sup>Y mutation does not affect a weak pyrethroid interaction with a glycine residue, which has a single hydrogen atom in the side chain.

Besides N<sup>1575</sup>Y, there are several other sodium channel mutations within LIII/IV that have been reported to be associated with pyrethroid resistance (Dong et al., 2014; Rinkevich et al., 2013). The frequent occurrence of mutations associated with pyrethroid resistance in this linker supports the allosteric interactions between IIS6 and LIII/IV in the sodium channel. For example, L<sup>1596</sup>P was found to be associated with pyrethroid resistance in varroa mites (Figure 5) (Dong et al., 2014). Although this mutation has not been functionally examined using varroa mite sodium channels expressed in *Xenopus* oocytes, insect sodium channels possess a proline at the corresponding position and the leucine substitution of proline in the cockroach sodium channel renders the cockroach sodium channel more sensitive to pyrethroids (Liu et al., 2006). Therefore, the L<sup>1596</sup>P mutation is predicted to make the varroa mite sodium channel more resistant to pyrethroids. Since L<sup>1596</sup>P alone could confer pyrethroid resistance, P1596, located at the C-terminus of LIII/IV, likely has a more drastic allosteric effect on pyrethroid binding (to PyR1 and/or PyR2) than N<sup>1575</sup>Y.

The involvement of other intracellular linkers in pyrethroid resistance has also been reported. E<sup>435</sup>K and C<sup>785</sup>R, in the linker connecting domains I and II (LI/II), were identified in pyrethroid resistant German cockroach populations (Liu et al., 2000). Like N<sup>1575</sup>Y, E<sup>435</sup>K or C<sup>785</sup>R alone did not reduce sodium channel sensitivity to pyrethroids. However, concurrence of either E<sup>435</sup>K or C<sup>785</sup>R mutation with the *kdr* mutations, V<sup>119(410)</sup>M in IS6 or L<sup>216(1014)</sup>F in IIS6, significantly increases pyrethroid resistance (Liu et al., 2002; Tan et al., 2002a). A mechanism similar to that for N<sup>1575</sup>Y could explain the role of E<sup>435</sup>K or C<sup>785</sup>R in pyrethroid resistance. Another example is G<sup>1111</sup> (in the cockroach sodium channel) in the second intracellular linker connecting domains II and III (LII/III), which is selectively involved in the response of sodium channels to type II

pyrethroids, such as deltamethrin (Du et al., 2009). Deletion of G<sup>1111</sup> (due to alternative splicing of cockroach sodium channel transcripts) makes cockroach sodium channels more resistant to type II pyrethroids. Interestingly, although the overall sequence of the intracellular linker is quite variable, the amino acid sequence around G<sup>1111</sup> is highly conserved among insect sodium channels. Two conserved lysine residues K<sup>1118</sup> and K<sup>1119</sup> downstream of G<sup>1111</sup> are also critical for the action of type II pyrethroids (Du et al., 2009). Neutralization of K<sup>1118</sup> and K<sup>1119</sup> confers resistance to type II pyrethroids. The precise mechanism through which these mutations selectively alter the interaction of sodium channels with pyrethroids remains unclear. It is possible that they alter the binding site for type II pyrethroids by an allosteric mechanism.

In conclusion, our study sheds light on the mechanism by which the N<sup>1575</sup>Y mutation enhances pyrethroid resistance and explains the molecular basis of the concurrence of N<sup>1575</sup>Y and L<sup>2i16(1014)</sup>F in pyrethroid-resistant mosquito populations. Furthermore, our findings provide evidence for possible allosteric, cross-domain interactions between transmembrane segments and intracellular loops of the sodium channel in mediating the action of pyrethroids on sodium channels.

## **Acknowledgements**

We thank Dr. Kris Silver for critical review of the manuscript. Computations were performed using the facilities of the Shared Hierarchical Academic Research Computing Network (SHARCNET, [www.sharcnet.ca](http://www.sharcnet.ca)).

MOL #94730

### **Authorship Contributions**

Participated in research design: Wang, Zhorov and Dong

Conducted experiments and performed data analysis: Wang, Du and Nomura

Wrote or contributed to the writing of the manuscript: Wang, Du, Liu, Zhorov and Dong

## References

- Catterall WA (2002) Molecular mechanisms of gating and drug block of sodium channels. *Novartis Found Symp* **241**: 206-218.
- Catterall WA (2012) Voltage - gated sodium channels at 60: structure, function and pathophysiology. *J Physiol* **590**(11): 2577-2589.
- Catterall WA, Cestele S, Yarov-Yarovoy V, Yu FH, Konoki K and Scheuer T (2007) Voltage-gated ion channels and gating modifier toxins. *Toxicon : official journal of the International Society on Toxicology* **49**(2): 124-141.
- Dong K, Du Y, Rinkevich F, Nomura Y, Xu P, Wang L, Silver K and Zhorov BS (2014) Molecular biology of insect sodium channels and pyrethroid resistance. *Insect Biochem Molec Biol* **50**: 1-17.
- Doyle DA, Cabral JM, Pfuetzner RA, Kuo A, Gulbis JM, Cohen SL, Chait BT and MacKinnon R (1998) The structure of the potassium channel: molecular basis of K<sup>+</sup> conduction and selectivity. *science* **280**(5360): 69-77.
- Du Y, Lee JE, Nomura Y, Zhang T, Zhorov B and Dong K (2009) Identification of a cluster of residues in transmembrane segment 6 of domain III of the cockroach sodium channel essential for the action of pyrethroid insecticides. *Biochem J* **419**: 377-385.
- Du Y, Nomura Y, Satar G, Hu Z, Nauen R, He SY, Zhorov BS and Dong K (2013) Molecular evidence for dual pyrethroid-receptor sites on a mosquito sodium channel. *Proc Natl Acad Sci U S A* **110**(29): 11785-11790.
- Enayati AA, Vatandoost H, Ladonni H, Townson H and Hemingway J (2003) Molecular evidence for a kdr-like pyrethroid resistance mechanism in the malaria vector mosquito *Anopheles stephensi*. *Med Vet Entomol* **17**:138-144.
- Garden DP and Zhorov BS. (2010) Docking flexible ligands in proteins with a solvent exposure- and distance-dependent dielectric function. *J Comput Aided Mol Des* **24**:91-105.
- Goldin AL (2003) Mechanisms of sodium channel inactivation. *Curr Opin Neurobiol* **13**(3): 284-290.
- Jones CM, Liyanapathirana M, Agossa FR, Weetman D, Ranson H, Donnelly MJ and Wilding CS (2012) Footprints of positive selection associated with a mutation (N1575Y) in the voltage-gated sodium channel of *Anopheles gambiae*. *Proc Natl Acad Sci* **109**(17): 6614-6619.
- Karunaratne SHPP, Hawkes NJ, Perera MDB, Ranson H and Hemingway J (2007) Mutated sodium channel genes and elevated monooxygenases are found in pyrethroid resistant populations of Sri Lankan malaria vectors. *Pestic Biochem Physiol* **88**: 108-113.
- Kasai S, Ng LC, Lam-Phua SG, Tang CS, Itokawa K, Komogata O, Kobayashi M and Tomita T (2011) First detection of a putative knockdown resistance gene in major mosquito vector, *Aedes albopictus*. *Jpn J Infect Dis* **64**: 217-221.
- Kawada H, Higa Y, Komagata O, Kasai S, Tomita T, Yen NT, Loan LL, Sánchez RAP and Takagi M (2009) Widespread distribution of a newly found point mutation in voltage-gated sodium channel in pyrethroid-resistant *Aedes aegypti* populations in Vietnam. *PLoS Neglected Tropical Diseases* **3**(10): e0000527.
- Kim H, Baek JH, Lee W-J and Lee S-H (2007) Frequency detection of pyrethroid resistance allele in *Anopheles sinensis* populations by real-time PCR amplification of specific allele (rtPASA). *Pestic Biochem Physiol* **87**: 54-61.
- Li Z and Scheraga HA (1987) Monte Carlo-minimization approach to the multiple-minima problem in protein folding. *Proc Natl Acad Sci USA* **84**:6611-6615.
- Lipkind GM and Fozzard HA (2005) Molecular modeling of local anesthetic drug binding by voltage-gated sodium channels. *Mol Pharmacol* **68**(6): 1611-1622.

- Liu Z, S.M. Valles, and K. Dong (2000) Novel point mutations in the German cockroach para sodium channel gene are associated with knockdown resistance (*kdr*) to pyrethroid insecticides. *Insect Biochem Molec Biol* **30**: 991-997.
- Liu Z, Tan J, Huang Z and Dong K (2006) Effect of a fluvalinate-resistance-associated sodium channel mutation from varroa mites on cockroach sodium channel sensitivity to fulvalinate, a pyrethroid insecticide. *Insect Biochem Molec Biol* **36**: 885-889.
- Liu Z, Tan J, Valles SM and Dong K (2002) Synergistic interaction between two cockroach sodium channel mutations and a tobacco budworm sodium channel mutation in reducing channel sensitivity to a pyrethroid insecticide. *Insect Biochem Molec Biol* **32**: 397-404.
- Long SB, Campbell EB and Mackinnon R (2005) Crystal structure of a mammalian voltage-dependent Shaker family K<sup>+</sup> channel. *Science* **309**(5736): 897-903.
- Luleypap HU, Alptekin D, Kasap H and Kasap M (2002) Detection of knockdown resistance mutations in *Anopheles sacharovi* (Diptera: Culicidae) and genetic distance with *Anopheles gambiae* (Diptera: Culicidae) using cDNA sequencing of the voltage-gated sodium channel gene. *J Med Entomol* **39**(6): 870-874.
- Martinez-Torrez D, Chandre F, Williamson M, Darriet F, Berge J, Devonshire A, Guillet P, Pasteur N and Pauron D (1998) Molecular characterization of pyrethroid knockdown resistance (*kdr*) in the major malaria vector *Anopheles gambiae* s.s. *Insect Mol Biol* **7**: 179-184.
- Narahashi T (1996) Neuronal ion channels as the target sites of insecticides. *Pharmacol Toxicol* **78**: 1-14.
- O'Reilly AO, Khambay BPS, Williamson MS, Field LA, Wallace BA and Davies TGE (2006) Modelling insecticide-binding sites in the voltage-gated sodium channel. *Biochem J* **396**: 255-263.
- O'Reilly AO, Williamson MS, Gonzalez-Cabrera J, Turberg A, Field LM, Wallace BA and Davies TG (2014) Predictive 3D modelling of the interactions of pyrethroids with the voltage-gated sodium channels of ticks and mites. *Pest management science* **70**(3): 369-377.
- Payandeh J, Scheuer T, Zheng N and Catterall WA (2011) The crystal structure of a voltage-gated sodium channel. *Nature* **475**: 353-359.
- Ranson H, Jensen B, Vulule JM, Wang X, Hemingway J and Collins FH (2000) Identification of a point mutation in the voltage-gated sodium channel gene of Kenyan *Anopheles gambiae* associated with resistance to DDT and pyrethroids. *Insect Mol Biol* **9**(5): 491-497.
- Rinkevich FD, Du Y and Dong K (2013) Diversity and Convergence of Sodium Channel Mutations Involved in Resistance to Pyrethroids. *Pestic Biochem Physiol* **106**(3): 93-100.
- Saavedra-Rodriguez K, Urdaneta-Marquez L, Rajatileka S, Moulton M, Flores AE, Fernandez-Salas I, Bisset J, Rodriguez M, McCall PJ, Donnelly MJ, Ranson H, Hemingway J and Black WCI (2007) A mutation in the voltage-gated sodium channel gene associated with pyrethroid resistance in Latin American *Aedes aegypti*. *Insect Molecular Biology* **16**(6): 785-798.
- Singh OP, Dykes CL, Das MK, Pradhan S, Bhatt RM, Agrawal OP and Adak T (2010) Presence of two alternative *kdr*-like mutations, L1014F and L1014S, and a novel mutation V1010L, in the voltage-gated Na<sup>+</sup> channel of *Anopheles culicifacies* from Orissa, India. *Malaria J* **9**: 146.
- Soderlund DM (2005) Sodium channels, in *Comprehensive molecular insect science* (Gilbert LI, Iatrou K and Gill SS eds) pp 1-24, Elsevier, Amsterdam.
- Stump AD, Atielli FK, Vulule JM and Besansky NJ (2004) Dynamics of the pyrethroid knockdown resistance allele in western Kenyan populations of *Anopheles gambiae* in response to insecticide-treated bed net trials. *Am J Trop Med Hyg* **70**(6): 591-596.
- Tan J, Liu Z, Tsai TD, Valles SM, Goldin AL and Dong K (2002a) Novel sodium channel gene mutations in *Blattella germanica* reduce the sensitivity of expressed channels to deltamethrin. *Insect Biochem Molec Biol* **32**: 445-454.
- Tan J, Z. Liu Z, Nomura Y, Goldin AL and Dong K (2002b) Alternative splicing of an insect sodium channel gene generates pharmacologically distinct sodium channels. *J Neurosci* **22**: 5300-5309.

- Tan WL, Li CX, Wang ZM, Liu MD, Dong YD, Feng XY, Wu ZM, Guo XX, Xing D, Zhang YM, Wang ZC and Zhao TY (2012) First detection of multiple knockdown resistance (*kdr*)-like mutations in voltage-gated sodium channel using three new genotyping methods in *Anopheles sinensis* from Guangxi Province, China. *J Med Entomol* **49**(5): 1012-1020.
- Tatebayashi H and Narahashi T (1994) Differential mechanism of action of the pyrethroid tetramethrin on tetrodotoxin-sensitive and tetrodotoxin-resistant sodium channels. *J Pharmacol Exper Therap* **270**: 595-603.
- Tikhonov DB and Zhorov BS (2007) Sodium channels: ionic model of slow inactivation and state-dependent drug binding. *Biophys J* **93**(5): 1557-1570.
- Tikhonov DB and Zhorov BS (2012) Architecture and pore block of eukaryotic voltage-gated sodium channels in view of NavAb bacterial sodium channel structure. *Mol Pharmacol* **82**(1): 97-104.
- Usherwood PNR, Davies TGE, Mellor IR, O'Reilly AO, Peng F, Vais H, Khambay BPS, Field LM and Williamson MS. (2007). Mutations in DIIS5 and the DIIS4-S5 linker of *Drosophila melanogaster* sodium channel define binding domains for pyrethroids and DDT. *FEBS Letters* **581**:5485-5492
- Vais H, Williamson MS, Goodson SJ, Devonshire AL, Warmke JW, Usherwood PNR and Cohen CJ (2000) Activation of *Drosophila* sodium channels promotes modification by deltamethrin: Reductions in affinity caused by knock-down resistance mutations. *J Gen Physiol* **115**(3): 305-318.
- Verhaeghen K, van Bortel W, Trung HD, Sochantha T, Keokenchanh K and Coosemans M (2010) Knockdown resistance in *Anopheles vagus*, *An. sinensis*, *An. paraliae* and *An. peditaeniatus* populations of the Mekong region. *Parasit Vect* **3**: 59.
- Vijverberg HPM, vanden Zalm JM and vanden Bercken J (1982) Similar mode of action of pyrethroids and DDT on sodium channel gating in myelinated nerves. *Nature* **295**: 601-603.
- Wang ZM, Li CX, Xing D, Yu YH, Liu N, Xue RD, Dong YD and Zhao TY (2012) Detection and widespread distribution of sodium channel alleles characteristic of insecticide resistance in *Culex pipiens* complex mosquitoes in China. *Med Vet Entomol* **26**: 228-232.
- Zhorov BS and Tikhonov DB (2004) Potassium, sodium, calcium and glutamate-gated channels: pore architecture and ligand action. *J Neurochem* **88**(4): 782-799.

## Footnotes

This study was supported by the National Institutes of Health National Institute of General Medicine [GM057440]; the National Institutes of Health National Institute of allergy and infectious diseases [R21AI090303]; and the Natural Sciences and Engineering Research Council of Canada [RGPIN-2014-04894].

## Figure legends

**Figure 1.** The topology of the sodium channel protein indicating the position of  $L^{2116(1014)}F/S/C/W$  and  $N^{1575}Y$  mutations. The sodium channel protein consists of four homologous domains (I-IV), each formed by six transmembrane segments (S1-S6) connected by intracellular and extracellular loops. Residue positions  $L^{1014}F$  and  $N^{1575}Y$  correspond to the housefly sodium channel (GenBank accession numbers: AAB47604 and AAB47605).  $L^{2116}F$  is labeled using the nomenclature that is universal for P-loop ion channels, in which a residue is labeled by the domain number (1 to 4), segment type (*k*, the L45 linker; *i*, the inner helix, i.e., S6; *o*, the outer helix, i.e., S5), and the relative number of the residue in the segment.

**Figure 2.**  $N^{1575}Y$  does not alter inactivation kinetics. (A) Representative current traces. The sodium currents were elicited by a 20-ms depolarization to 0 mV from the holding potential of -120 mV. (B) Voltage dependence of the sodium current decay. Time constant of sodium current decay was calculated by fitting the decaying part of current traces, elicited by a series of depolarizing voltages, with a single exponential function.

**Figure 3.** The  $L^{1014}F+N^{1575}Y$  double mutation reduced the sensitivity of AaNa<sub>v</sub>1-1 channels to permethrin and deltamethrin. (A) – (D), Tail currents induced by permethrin (1 μM) in AaNa<sub>v</sub>1-1 (A),  $N^{1575}Y$  (B),  $L^{1014}F$  (C), and  $L^{1014}F+N^{1575}Y$  (D) channels. (E) and (F), Percentage of channel modification by permethrin (E) and deltamethrin (F) of wild-type and mutant channels. Percentage of channels modified by pyrethroids was calculated as described in the Materials and Methods. The values of EC<sub>20</sub> for permethrin were 0.12, 0.18, 1.0 and 9.8 μM for AaNa<sub>v</sub>1-1,  $N^{1575}Y$ ,  $L^{1014}F$ , and  $L^{1014}F+N^{1575}Y$  channels, respectively. The values of EC<sub>20</sub> for deltamethrin were 0.1, 0.11, 1.4, and 5.3 μM for AaNa<sub>v</sub>1-1,  $N^{1575}Y$ ,  $L^{1014}F$ , and  $L^{1014}F+N^{1575}Y$  channels, respectively.

The number of oocytes for each mutant construct was >5. Each data point indicates mean  $\pm$  SEM. Asterisks indicate significant differences from the AaNa<sub>v</sub>1-1 channel as determined by using one-way analysis of variance with Scheffe's post hoc analysis, and significant values were set at  $P < 0.05$ .

**Figure 4.** N<sup>1575</sup>Y enhanced resistance to pyrethroids caused by L1014S/W. Effects of L1014S/W (A, B and C, D, respectively) mutations on the sensitivity of AaNa<sub>v</sub>1-1 channels to permethrin (A, C) or deltamethrin (B, D). Percentages of channel modification by permethrin or deltamethrin were determined using the method described in the Materials and Methods. The number of oocytes for each mutant construct was >5. Each data point indicates mean  $\pm$  SEM. Asterisks indicate significant differences from the AaNa<sub>v</sub>1-1 channel as determined by using one-way analysis of variance with Scheffe's post hoc analysis, and significant values were set at  $P < 0.05$ .

**Figure 5.** N<sup>1575</sup>Y did not enhance pyrethroid resistance caused by other mutations examined in this study. **A.** The positions of the mutations in the sodium channel protein. The amino acid sequence of the linker connecting domains III and IV is shown below the topology, The MFMT motif, which is critical for fast inactivation, is underlined. The N<sup>1575</sup>Y mutation is marked in bold. Residue P<sup>1596</sup> in this linker, whose leucine substitution was previously confirmed to increase pyrethroid potency, is also shown in bold. **B and C.** Effects of N<sup>1575</sup>Y on the sensitivity of AaNa<sub>v</sub>1-1 wild-type and mutant channels to 1  $\mu$ M permethrin (B) and 1  $\mu$ M deltamethrin (C). The number of oocytes for each mutant construct was >5. Each data point indicates mean  $\pm$  SEM. The percentage of channel modification for all mutant channels except N<sup>1575</sup>Y was significantly different from that of the AaNa<sub>v</sub>1-1 channel, but no significant difference between the double

mutants and their respective singles, as determined by using one-way analysis of variance with Scheffe's post hoc analysis, and significant values were set at  $P < 0.05$ .

**Figure 6.**  $K_v1.2$ -based model of the open  $AaNa_v1-1$  channel with deltamethrin bound to PyR2.

**A-B**, Side (**A**) and cytoplasmic (**B**) views. Deltamethrin is shown by sticks with green carbons, red oxygens, gray hydrogens, and brown bromine atoms. Semi-transparent cyan, pink, yellow, and green surfaces show pyrethroid-sensing residues in helices IL45, IS6, IIS6, and IIS6, respectively.

Note that helix IIS6 contributes residue  $L^{2i16}$  to PyR2 and may contribute residue  $V^{2i18}$  to PyR1 which contains  $F^{3i16}$  in helix IIS6. **C-F**, Cytoplasmic view along helix IIS6 of models of  $AaNa_v1-1$  mutants  $L^{1i18}G$  (**C**),  $L^{2i16}G$  (**D**),  $L^{2i16}S$  (**E**), and  $L^{2i16}F$  (**F**) of the open  $AaNa_v1-1$  channel with deltamethrin bound in the pyrethroid PyR2. The long flexible side chain of  $L^{2i16}$  in the  $L^{1i18}G$  mutant (**C**) and the wild-type channel (**B**) favorably interact with the ligand and a small shift of helix IIS6 upon mutation  $N^{1575}Y$  would have little effect on this interaction. The ligand potency in the  $L^{2i16}G$  mutant (**D**) would also have low-sensitivity to the IIS6 shift because the tiny side chain of  $G^{2i16}$  is located rather far from the ligand. However, the IIS6 shift would deteriorate unfavorable interactions of the hydrophilic  $S^{2i16}$  with the hydrophobic ligand (**E**) or would cause an unfavorable clash of deltamethrin with the big and inflexible  $F^{2i16}$  (**D**).

#### Data Supplement PDB file captions

**Model1 .  $L^{2i16}$  temp.pdb.** Model of the deltamethrin-bound  $AaNa_v1-1$  wild-type channel.

**Model2 .  $L^{2i16}F$  temp.pdb.** Model of the deltamethrin-bound  $L^{2i16}F$  channel.

**Model3 .  $L^{2i18}G$  temp.pdb.** Model of the deltamethrin-bound  $L^{2i18}G$  channel.

**Model4 .  $L^{2i16}G$  temp.pdb.** Model of the deltamethrin-bound  $L^{2i16}G$  channel.

MOL #94730

**Model5. L<sup>2i16</sup>S temp.pdb.** Model of the deltamethrin-bound L<sup>2i16</sup>S channel.

**Table 1**

Voltage dependence of activation and fast inactivation of AaNa<sub>v</sub>1-1 and its mutants.

The voltage-dependence of conductance and inactivation data were fitted with two-state Boltzmann equations, as described in Materials and Methods, to determine  $V_{1/2}$ , the voltage for half-maximal conductance or inactivation and  $k$ , the slope for conductance or inactivation. Each value represents the mean  $\pm$  SEM.

	Activation		Fast Inactivation		
	$V_{1/2}$ (mV)	$k$	$V_{1/2}$ (mV)	$k$	n
AaNa <sub>v</sub> 1-1	-33.6 $\pm$ 1.1	5.7 $\pm$ 0.3	-53.7 $\pm$ 0.6	5.0 $\pm$ 0.1	19
N <sup>1575</sup> Y	-32.3 $\pm$ 1.6	6.6 $\pm$ 0.3	-56.5 $\pm$ 0.5	5.0 $\pm$ 0.1	20
L <sup>2i16(1014)</sup> F	-31.3 $\pm$ 0.9	4.0 $\pm$ 0.3	-49.6 $\pm$ 0.4	4.5 $\pm$ 0.1	10
L <sup>2i16(1014)</sup> F+N <sup>1575</sup> Y	-28.6 $\pm$ 1.1	5.6 $\pm$ 0.2	-51.1 $\pm$ 0.4	4.8 $\pm$ 0.1	27
L <sup>2i16(1014)</sup> S	-36.3 $\pm$ 1.1	4.3 $\pm$ 0.3	-50.0 $\pm$ 0.3	4.7 $\pm$ 0.1	11
L <sup>2i16(1014)</sup> S+N <sup>1575</sup> Y	-33.8 $\pm$ 1.2	5.1 $\pm$ 0.4	-51.5 $\pm$ 0.7	4.9 $\pm$ 0.1	10
L <sup>2i16(1014)</sup> W	-30.2 $\pm$ 1.1	5.0 $\pm$ 0.2	-50.3 $\pm$ 0.5	4.8 $\pm$ 0.1	6
L <sup>2i16(1014)</sup> W+N <sup>1575</sup> Y	-29.8 $\pm$ 1.2	5.2 $\pm$ 0.2	-53.2 $\pm$ 0.6	5.1 $\pm$ 0.1	5
L <sup>2i16(1014)</sup> G	-31.5 $\pm$ 1.0	4.9 $\pm$ 0.3	-48.9 $\pm$ 0.7	4.7 $\pm$ 0.1	7
L <sup>2i16(1014)</sup> G+N <sup>1575</sup> Y	-34.2 $\pm$ 1.2	5.0 $\pm$ 0.4	-52.3 $\pm$ 0.6	4.6 $\pm$ 0.1	9
L <sup>2i16(L1014)</sup> C	-37.5 $\pm$ 1.1	6.2 $\pm$ 0.3	-51.8 $\pm$ 0.5	5.0 $\pm$ 0.1	5
V <sup>2i18(1016)</sup> G	-33.0 $\pm$ 1.0	5.3 $\pm$ 0.3	-51.8 $\pm$ 0.5	5.6 $\pm$ 0.1	6
V <sup>2i18(1016)</sup> G+N <sup>1575</sup> Y	-35.4 $\pm$ 1.1	5.6 $\pm$ 0.2	-52.1 $\pm$ 0.7	5.3 $\pm$ 0.1	7

MOL #94730

L <sup>1i18</sup> G	-30.1 ± 1.0	4.8 ± 0.5	-49.2 ± 0.6	4.9 ± 0.1	8
L <sup>1i18</sup> G+N <sup>1575</sup> Y	-32.5 ± 1.2	4.9 ± 0.4	-50.0 ± 0.5	4.9 ± 0.1	6
L <sup>1i18</sup> F	-29.7 ± 1.0	3.9 ± 0.1	-42.9 ± 0.7	5.0 ± 0.1	8
L <sup>1i18</sup> F+N <sup>1575</sup> Y	-30.7 ± 0.5	4.0 ± 0.2	-44.2 ± 0.6	5.2 ± 0.1	7
L <sup>1i18</sup> W	-29.0 ± 1.1	4.2 ± 0.2	-48.4 ± 0.2	5.2 ± 0.1	5
L <sup>1i18</sup> W+N <sup>1575</sup> Y	-28.2 ± 0.6	4.8 ± 0.2	-53.3 ± 0.6	5.4 ± 0.1	8
S <sup>1i29</sup> A	-33.2 ± 1.0	5.2 ± 0.3	-51.2 ± 0.5	5.2 ± 0.1	5
S <sup>1i29</sup> A+N <sup>1575</sup> Y	-32.0 ± 1.2	5.0 ± 0.2	-50.2 ± 0.6	5.1 ± 0.1	6

---

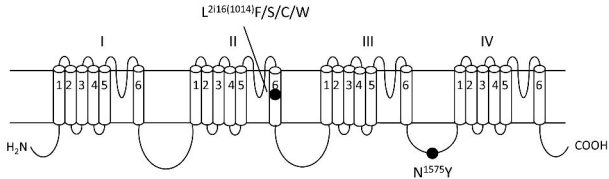
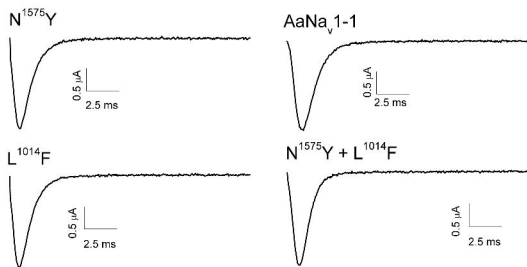


Figure 1

A



B

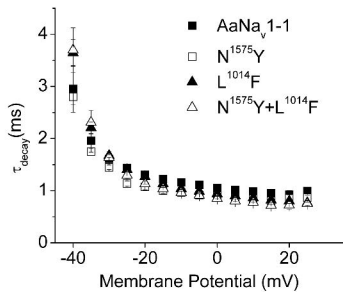


Figure 2

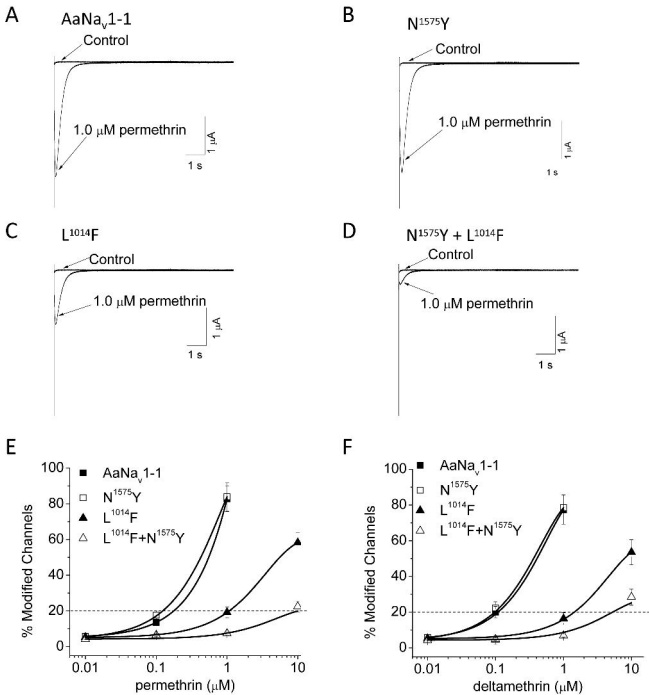
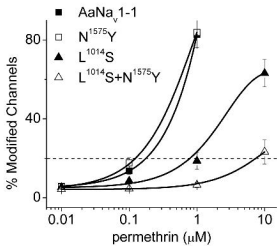
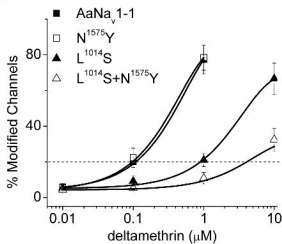


Figure 3

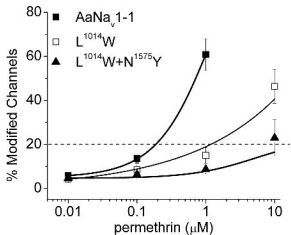
A



B



C



D

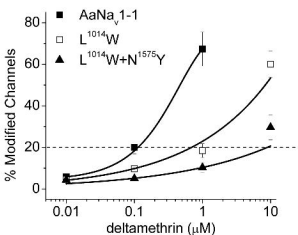
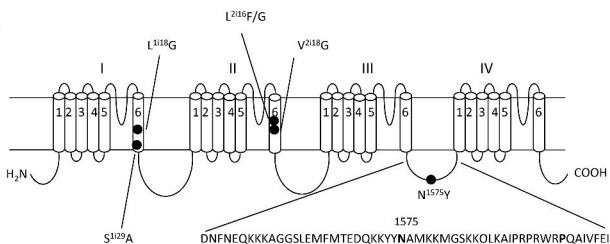
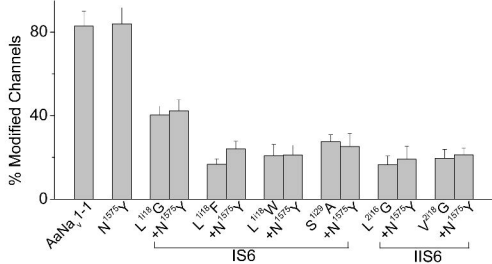


Figure 4

A



B



C

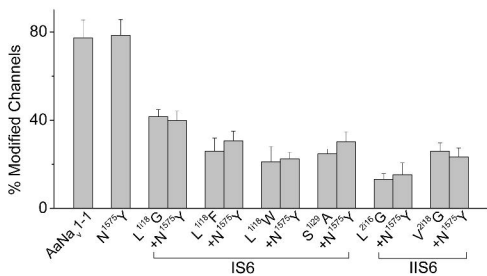


Figure 5

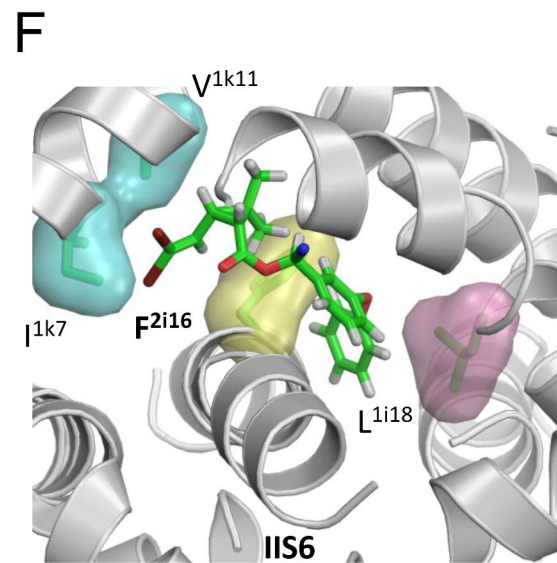
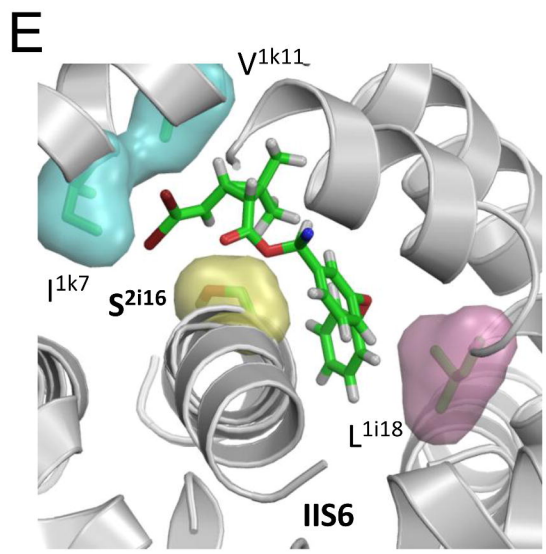
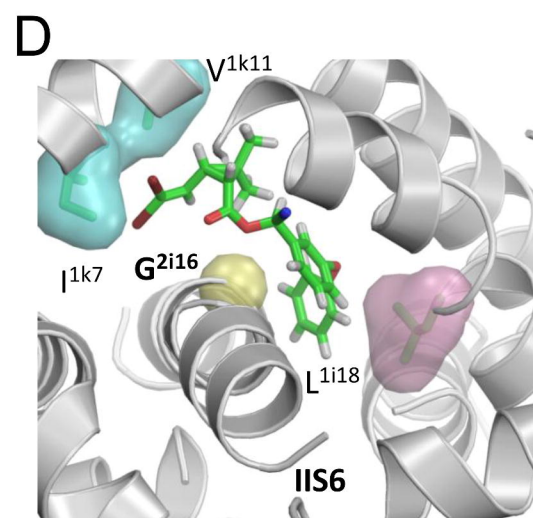
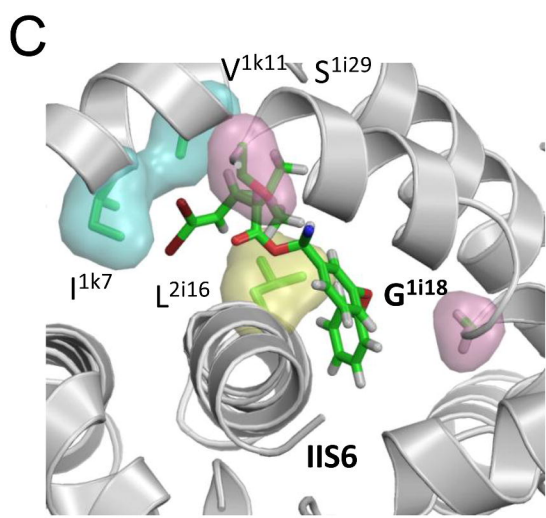
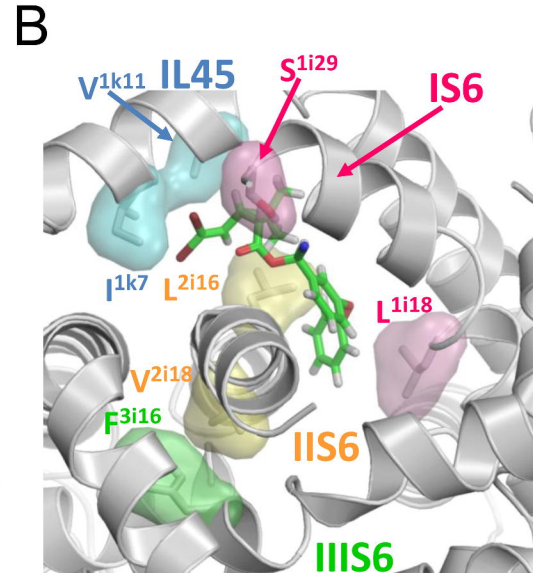
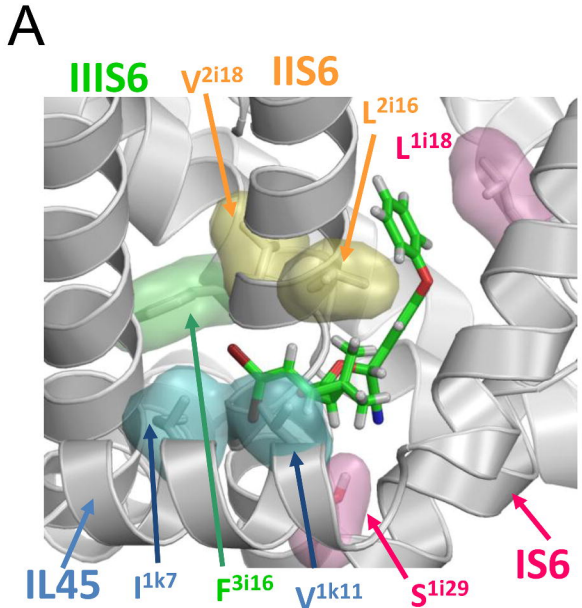


Figure 6

Molecular Pharmacology

Supplemental information accompanying the manuscript

**A mutation in the intracellular loop III/IV of mosquito sodium channel synergizes  
the effect of mutations in helix IIS6 on pyrethroid resistance**

By

Lingxin Wang, Yoshiko Nomura, Yuzhe Du, Nannan Liu, Boris Zhorov, Ke Dong

Department of Entomology, Genetics and Neuroscience Programs, Michigan State  
University, East Lansing, MI, USA (L.W., Y.N., Y.D,K.D.)

Department of Entomology and Plant Pathology; Auburn University, Auburn,  
Alabama, USA (N.L.)

Department of Biochemistry and Biomedical Sciences, McMaster University,  
Hamilton, Ontario, Canada (B.S.Z.)

Sechenov Institute of Evolutionary Physiology & Biochemistry, Russian Academy of  
Sciences, St. Petersburg (B.S.Z.)

**IS5**

AaNa<sub>v</sub>1 272DVIILTMTFSLSVFALMGLQIYMGVLT  
 AgNa<sub>v</sub>1 .....

**IS6**

AaNa<sub>v</sub>1 403HMLFFIVIIFLGSFYLVNLILAI  
 AgNa<sub>v</sub>1 .....

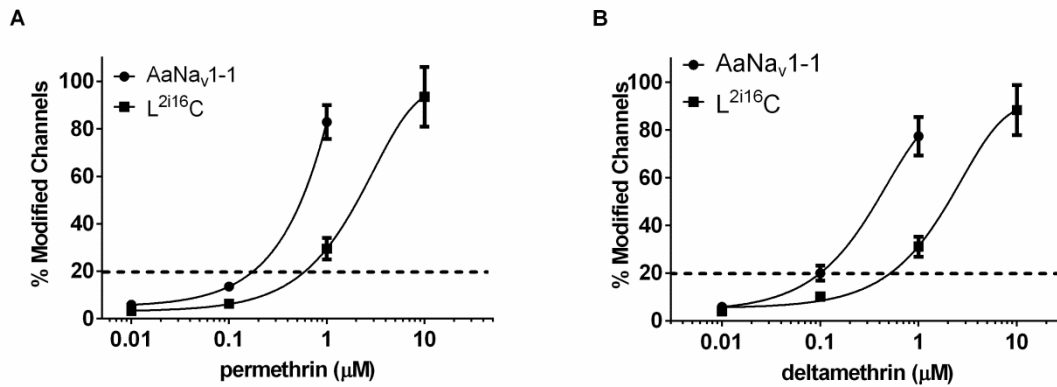
**IIS6**

AaNa<sub>v</sub>1 1006VSCIPFFLATVVIGNLVGLNLFALLL  
 AgNa<sub>v</sub>1 .....V.....

**LIII/IV**

AaNa<sub>v</sub>1 1579IDNFNEQKKKAGGSLEMFMTEDQKKYYNAMKKMGSKKPLKAI PRPRWRPQAI VFEI  
 AgNa<sub>v</sub>1 .....

**Supplemental Figure 1.** Amino acid sequence alignment of IS5, IS6, IIS6 and LIII/IV of Na<sub>v</sub> channels AgNa<sub>v</sub>1 and AaNa<sub>v</sub>1 from *Anopheles gambiae* and *Aedes aegypti*, respectively. The sequences are from the GenBank with accession numbers of AM422833 for AgNa<sub>v</sub>1 and EU399181 for AaNa<sub>v</sub>1. The residues in AgNa<sub>v</sub>1 that are identical to those in AaNa<sub>v</sub>1 are marked with dots. The position of the first amino acid residue is indicated in AaNa<sub>v</sub>1 sequences.



**Supplemental Figure 2.** The L<sup>2i16</sup>C (i.e., L1014C) mutation significantly reduced the sensitivity of AaNa<sub>v</sub>1-1 channels to permethrin and deltamethrin. Percentage of channel modification by permethrin (A) and deltamethrin (B) was calculated as described in the Materials and Methods. The values of EC<sub>20</sub> for permethrin are 0.11 and 0.4 μM for AaNa<sub>v</sub>1-1 and L<sup>2i16</sup>C channels, respectively. The values of EC<sub>20</sub> for deltamethrin are 0.1 and 0.42 μM for AaNa<sub>v</sub>1-1 and L<sup>2i16</sup>C channels, respectively.

